Temperature-Driven Changeover in the Electron-Transfer Mechanism of a Thermophilic Plastocyanin

ARTICLE *in* JOURNAL OF PHYSICAL CHEMISTRY LETTERS · MARCH 2014

Impact Factor: 7.46 · DOI: 10.1021/jz500150y

THE JOURNAL OF PHYSICAL CHEMISTRY Letters

Letter

pubs.acs.org/JPCL

Temperature-Driven Changeover in the Electron-Transfer Mechanism of a Thermophilic Plastocyanin

José Luis Olloqui-Sariego,*[,†] Blas Moreno-Beltrán,[‡] Antonio Díaz-Quintana,[‡] Miguel A. De la Rosa,[‡] Juan José Calvente,[†] and Rafael Andreu[†]

[†]Departamento de Química Física, Universidad de Sevilla, c/Profesor García González, 1, 41012 Sevilla, Spain

[‡]Instituto de Bioquímica Vegetal y Fotosíntesis, cicCartuja, Universidad de Sevilla y C.S.I.C, Avd. Américo Vespucio 49, 41092 Sevilla, Spain

Supporting Information

ABSTRACT: Electron-transfer kinetics of the thermophilic protein Plastocyanin from *Phormidium laminosum* adsorbed on 1,ω-alkanedithiol self-assembled monolayers (SAMs) deposited on gold have been investigated. The standard electron-transfer rate constant has been determined as a function of electrode−protein distance and solution viscosity over a broad temperature range (0−90 °C). For either thin or thick SAMs, the electron-transfer regime remains invariant with temperature, whereas for the 1,11-undecanethiol SAM of intermediate chain length, a kinetic regime changeover from a gated or friction-controlled mechanism at low temperature (0−30 °C) to a nonadiabatic mechanism above 40 °C is observed. To the best of our knowledge, this is the first time a thermal-induced transition between these two kinetic regimes is reported for a metalloprotein.

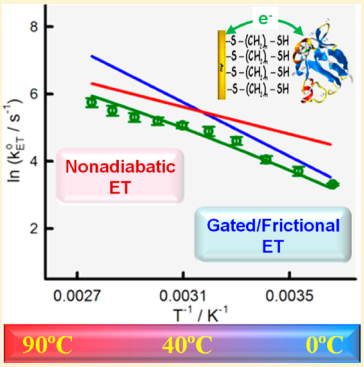

SECTION: Surfaces, Interfaces, Porous Materials, and Catalysis

Several strategies have been proposed to elucidate the factors that determine the rate of electron exchange between proteins and electrodes. Among them, the analysis of the effects of the protein−electrode distance, temperature, or solution viscosity on the electron-transfer (ET) rate constant stand out.[1−5] These studies have revealed two distinct kinetic regimes, in which ET rates are either independent or exponentially dependent on the protein−electrode distance. This last regime is well-described by a nonadiabatic ET mechanism, where the ET rate is controlled by the electron tunneling frequency at the top of the activation barrier.[5−15] However, the nature of the rate-limiting event is more ambiguous for the distance-independent kinetic regime, for which two alternatives have been purported in the literature. The first assumes that, as a consequence of the increased electronic coupling at short protein−electrode distances, the ET rate is controlled by a frictional mechanism that involves the protein and its surrounding medium and takes the reactant to the top of the activation barrier.[16−31] The second introduces a preceding barrier-crossing event (gating step), which may involve a conformational fluctuation[32] or a protein reorientation,[33] to optimize the rate of ET.[32−39] Irrespective of the precise nature of the controlling event in the distance-independent kinetic regime, the transition between the two kinetic regimes has been demonstrated by varying systematically the strength of the electronic coupling between the electrode and protein by using molecular spacers of variable composition and length. For redox proteins immobilized on thiol monolayers ($HS-(CH_2)_n-X$), the mechanism transition has often been reported to take place for a protein−electrode distance corresponding to $n \approx 10$.[12,15,24,25,31,33,39−43] Moreover, each kinetic regime can be further characterized by a distinct dependence of the ET rate constant on the temperature and solution viscosity,[25−33,44,45] though temperature- or viscosity-driven mechanism transitions have not yet been reported for metalloproteins. To the best of our knowledge, the current work provides the first observation of a temperature-induced mechanism changeover for a redox metalloprotein.

Thermal studies of typical redox proteins are significantly restrained because proteins become often denatured at moderate temperatures. A general approach to overcome this limitation would involve the use of thermophilic proteins that are likely to keep their structure and functionality intact in a broad temperature range. Within this context, we have previously reported on how Plastocyanin from *Phormidium laminosum* (Pc-PhoWT) adsorbed onto a graphite electrode displays an unusual thermal resistance, retaining its redox activity at temperatures as high as 90 °C.[46] Pc-PhoWT is a blue copper protein with a type-I redox center. The metal atom is buried in a hydrophobic pocket, and it is coordinated by two histidines (HisN and HisC), one methionine and one cysteine. The Cu binding site features a distorted trigonal pyramid, and

Received: January 23, 2014
Accepted: February 17, 2014

   dx.doi.org/10.1021/jz500150y | J. Phys. Chem. Lett. 2014, 5, 910−914

HisC is the only solvent-exposed copper ligand, thus making this group the most probable physiological ET port of the protein (see the Supporting Information). Its thermostability has also been probed by spectroscopic techniques in a broad temperature range.[47,48] On the basis of these findings, this protein appears to be a good candidate to assess the influence of temperature on its ET kinetics. Herein, we report on the effect of a broad variation of temperature (0−90 °C) on the ET kinetics of Pc-PhoWT immobilized on gold electrodes modified with 1,ω-alkanedithiol self-assembled monolayers (SAMs), under variable conditions of protein−electrode distance and solution viscosity. We provide clear experimental evidence of a changeover in the ET regime along a thermal scan when Pc-PhoWT is immobilized on a 1,11-undecanedithiol monolayer. In this case, electron exchange proceeds through the distance-independent kinetic limit at low temperatures, and it switches reversibly into the nonadiabatic regime as the temperature is raised over 40 °C.

The redox properties of Pc-PhoWT immobilized on distinct 1,ω-alkanedithiol SAMs differing in their hydrocarbon chain length were characterized by recording its voltammetric response as a function of scan rate. Figure S-2 (Supporting Information) illustrates some typical raw voltammograms. The formal potential (E^0) shifts from 0.421 to 0.375 V versus SHE upon increasing the dithiol chain length, remaining somewhat more positive than the reported values for Pc-PhoWT adsorbed onto graphite[46] and in solution.[48] A parallel variation of the reduction entropy (see the Supporting Information) toward less negative values suggests that the E^0 shift results from a tighter hydrophobic interaction between the protein and monolayer as the alkanedithiol chain length increases. To determine the standard ET rate constant (k_{ET}^0), the effect of the scan rate on the peak potential separation was assessed at distinct temperatures and electrode−protein distances. Accordingly, upon increasing the scan rate, the two voltammetric peaks depart from each other, producing trumpet plots as those depicted in Figure S-2 (Supporting Information). Solid lines in these plots are theoretical fits computed in the high reorganization energy limit of the Marcus ET theory (i.e., for $\lambda > F|E_p - E^0|$, where λ is the reorganization energy, E_p the peak potential, and F the Faraday's constant).[9] Though significant protein loss (~50%) was evident after exposing the electrode to the hottest solutions, a full recovery of the initial kinetic and thermodynamic ET parameters (see the Supporting Information) was observed after subjecting the immobilized protein to broad changes of temperature and solvent viscosity.

The effect of the electrode−protein distance on k_{ET}^0 at distinct temperatures is illustrated in Figure 1. At a given temperature (Figure 1a), it displays a biphasic behavior; the standard ET rate constant barely depends on the chain length up to ~9 methylene units but decays exponentially for the longer chain lengths ($n \geq 11$). The exponential decay factor is β = 1.14 per methylene group, consistent with the use of saturated hydrocarbon spacers.[49,50] Furthermore, Figure 1b shows that the temperature dependence of k_{ET}^0 is stronger at the plateau than that within the exponential decay region.

In the nonadiabatic limit (distance-dependent regime), the standard rate constant k_{ET}^0 is limited by the electron tunneling probability and can be expressed as

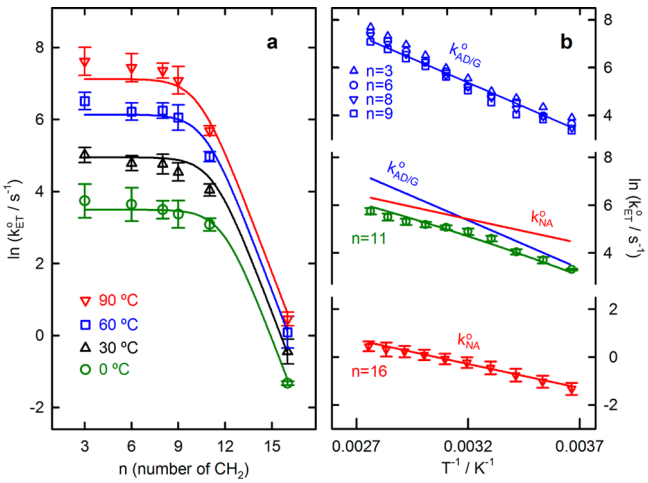

Figure 1. (a) Dependence of the logarithm of the standard ET rate constant on the number of methylene groups per thiol molecule for Pc-PhoWT immobilized on 1,ω-alkanedithiol SAMs, obtained in a 0.1 M sodium phosphate buffer of pH 7 at the indicated temperatures. Solid lines have been computed from eqs 1−4 in the text. (b) Arrhenius plots in the 0−90 °C temperature range. The green line in the n = 11 plot was computed from the corresponding red and blue lines according to eq 4, as indicated in the text. Symbols are experimental values, and error bars are standard deviations for at least three replicated measurements for each data point.

$$k_{NA}^0 = \frac{|H_{AB}^o|^2 \rho_m}{\hbar}\left(\frac{\pi^3 R}{\lambda}\right)^{1/2} \sqrt{T}\, \exp(-\beta n)\, \exp\left(-\frac{\lambda/4}{RT}\right) \quad (1)$$

where H_{AB}^o is the electronic coupling energy for n = 0 and ρ_m is the density of electronic states of the metal. Fit of eq 1 to experimental ln k_{ET}^0 versus T^{-1} data for n = 16 with β = 1.14 and ρ_m = 0.28 eV^{-1}[25] gives rise to λ = 61.7 kJ mol^{-1} (or 0.64 eV) and H_{AB}^o = 7 × 10^{-3} eV. The obtained value for λ falls within the range of accepted values for blue copper proteins.[46,51−54]

On the other hand, the standard rate constant under the distance-independent regime can be expressed as

$$k_{AD}^0 = \frac{1}{\tau_{eff}^o}\left(\frac{\lambda}{\pi^3 R}\right)^{1/2} \frac{1}{\sqrt{T}} \times \exp\left(-\frac{(\lambda/4) - |H_{AB}^o|e^{-\beta n} + \Delta H_\eta^\#}{RT}\right) \quad (2)$$

when the ET kinetics are controlled by a frictional mechanism or simply as

$$k_G^0 = A_G \exp\left(-\frac{\Delta H_G^\#}{RT}\right) \quad (3)$$

when they are controlled by a gating step. τ_{eff}^o is the high-temperature limit of the characteristic polarization relaxation time of the solvent/protein/SAM environment, $\Delta H_\eta^\#$ is the activation enthalpy associated with solvent/protein/SAM friction, and A_G and $\Delta H_G^\#$ are the Arrhenius preexponential factor and height of the activation barrier of the gating step, respectively.

Fit of eq 2 or 3 to the experimental ln k_{ET}^0 versus T^{-1} data for $n \leq 9$ (Figure 1b) gives rise to τ_{eff}^o = 7 × 10^{-9} s and $\Delta H_\eta^\#$ = 19.1 kJ mol^{-1} or A_G = 1.2 × 10^8 s^{-1} and $\Delta H_G^\#$ 34.5 kJ mol^{-1}, respectively. Bearing in mind that $\tau_{eff} = \tau_{eff}^o \exp(\Delta H_\eta^\#/RT)$, τ_{eff}

dx.doi.org/10.1021/jz500150y | J. Phys. Chem. Lett. 2014, 5, 910−914

shows a 10-fold decrease from ~32 at 0 °C to ~3.9 μs at 90 °C. The magnitude of these relaxation times is much larger than those of typical liquids[55] and ~10-fold the characteristic relaxation time reported by Khoshtariya et al.[25] for the adiabatic ET of cytochrome *c* adsorbed on thiol monolayers. On the other hand, this ~10 μs time scale lies well within the $1-10^3$ μs range that has been determined[56] for the mobility of the $\beta_7-\beta_8$ loop of the Plastocyanin from *Anabaena variabilis*. It should be noted that this loop contains three of the four copper ligands and, therefore, seems to be relevant for the ET process.

When the protein is adsorbed on a SAM with an intermediate alkyl chain length (n = 11), the $\ln k^0_{ET}$ versus T^{-1} slope changes from that characteristic of the distance-independent regime, at low temperatures, to that of the nonadiabatic regime at high temperatures. This transition can be accounted for with the following series combination of k^0_{NA} and $k^0_{AD/G}$ (green solid line in Figure 1b)

$$\frac{1}{k^0_{ET}} = \frac{1}{k^0_{NA}} + \frac{1}{k^0_{AD/G}} \quad (4)$$

which is known to describe the transition from the nonadiabatic to the adiabatic kinetic regimes,[25] but it can also account for the presence of a gating step[32] (see the Supporting Information). As the crossing point of the two individual k^0_{NA} and $k^0_{AD/G}$ contributions to k^0_{ET} shows (Figure 1b), the transition between the two limiting kinetic regimes takes place at ~40 °C for the n = 11 monolayer. It should be noted that this transition is predicted to be outside of the available temperature range for n < 11 or > 11 (Figure S-7 in the Supporting Information).

As a test of consistency, eq 4 was able to reproduce the experimental $\ln k^0_{ET}$ versus n dependence in Figure 1a with the same parameter values that were determined from the analysis of Figure 1b.

In order to corroborate the temperature-induced mechanistic changeover found for Pc-PhoWT adsorbed on the n = 11 SAM, use was made of the distinct sensitivity of the nonadiabatic and distance-independent kinetic regimes to changes in the solution viscosity η. Previous studies have shown that k^0_{NA} is independent of η, while $k^0_{AD/G}$ is proportional to $\eta^{-\gamma}$, where γ > 0.[25,33,57] Thus, according to eq 4, k^0_{ET} is expected to be proportional to $\eta^{-\gamma_{ap}}$, where the value of the γ_{ap} exponent ($0 < \gamma_{ap} \leq \gamma$) depends on the relative contributions of k^0_{NA} and $k^0_{AD/G}$ to k^0_{ET}.

Figure 2a illustrates the observed dependence of k^0_{ET} on the viscosity of aqueous glucose solutions, under variable conditions of electrode–protein distance and temperature. It can be observed that the slope of the logarithmic plot (i.e., γ_{ap}) decreases upon increasing the SAM thickness from $\gamma_{ap} \approx 1.1$ for n = 8 to $\gamma_{ap} \approx 0.0$ for n = 16, in agreement with the change of the kinetic regime discussed previously. More importantly, the slopes corresponding to the intermediate n = 11 SAM display a continuous variation with temperature from γ_{ap} = 0.77 at 10 °C to γ_{ap} = 0.09 at 70 °C (Figure 2b), as expected for a changeover of the ET mechanism from the frictional/gating regime to the nonadiabatic one. In order to quantify the γ value, corresponding to the $k^0_{AD/G}$ term, we have plotted in Figure 2c the difference between observed $1/k^0_{ET}$ and calculated $1/k^0_{NA}$ as a function of solution viscosity, where the k^0_{NA} values have been computed from eq 1 with the parameter values determined previously. According to eq 4, the ordinate values in these plots correspond to those of $1/k^0_{AD/G}$. The linearity of

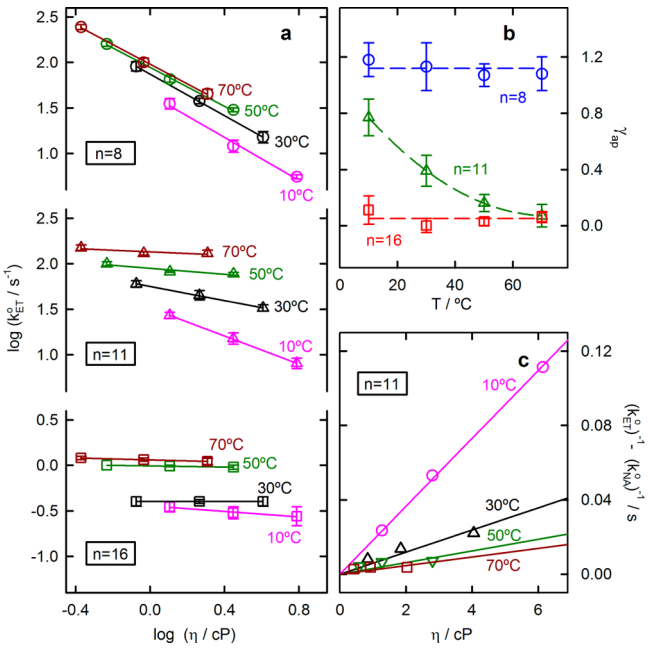

Figure 2. (a) Double-logarithmic plot of the overall standard ET rate constant for Pc-PhoWT immobilized on 1,ω-alkanedithiol SAMs, obtained in a 0.1 M sodium phosphate buffer of pH 7, against solution viscosity for the indicated temperature and spacer's number of methylene groups. (b) Slopes of the log k^0_{ET} versus log η plots in (a) as a function of temperature. (c) Difference between the reciprocals of the observed and calculated nonadiabatic standard ET rate constants as a function of solution viscosity for n = 11 and the indicated temperatures. Solid lines are least-squares linear fits passing through the origin.

these plots strongly suggests that the frictional coupling to the medium is very strong, with a real γ value close to 1.

Previous reports describing the transition between frictional/gating and nonadiabatic ET mechanisms for immobilized cytochrome *c*[25] and azurin[31] took advantage of the high sensitivity of the nonadiabatic ET rate to the electrode–protein distance. Herein, we have shown that the same transition can be achieved by exploiting the difference in the activation enthalpies of these two mechanisms. Once an adequate tunneling distance is selected, so that the values of the frictional/gating and nonadiabatic rate constants become similar at intermediate temperatures, the kinetic control can then be switched reversibly between the frictional/gating and nonadiabatic limits by just varying the temperature. In the case of the thermophilic plastocyanin from *Phormidium laminosum* adsorbed on a 1,11-undecanedithiol SAM, the mechanistic changeover takes place at 40 °C. This transition results from the interplay between different contributions to the observed ET rate, and our previous analysis helps to identify some physical prerequisites, such as the necessary difference in activation enthalpy between the two kinetic regimes or the importance of an adequate choice of the tunneling distance, to observe similar transitions for other redox proteins.

■ ASSOCIATED CONTENT

Supporting Information

Materials and methods. Structure of plastocyanin from *Phormidium laminosum*. Typical cyclic voltammograms and trumpet plots. Thermal stability of the SAM and the immobilized Pc-PhoWT. Expressions for the rate constants.

dx.doi.org/10.1021/jz500150y | J. Phys. Chem. Lett. 2014, 5, 910–914

Individual contributions to the ET rate constant. Thermodynamics of the immobilized Pc-PhoWT. This material is available free of charge via the Internet at http://pubs.acs.org.

AUTHOR INFORMATION

Corresponding Author

*E-mail: jlolloqui@us.es.

Notes

The authors declare no competing financial interest.

ACKNOWLEDGMENTS

J.L.O.-S., J.J.C., and R.A. acknowledge financial support from the DGICYT under Grant CTQ 2008-00371 and from the Junta de Andalucía under Grant P07-FQM-02492. B.M.-B., A.D.-Q., and M.A.D.l.R. recognize Funding Grant P06-CVI-01713 from Junta de Andalucía and DGICYT (BFU2012-31670/BMC). B.M.-B acknowledges a Ph.D. fellowship from the M.E.C.D. (AP2009/4092) is cofunded by the E.S.F.−E.R.F.

REFERENCES

(1) Fedurco, M. Redox Reactions of Heme-Containing Metalloproteins: Dynamic Effects of Self-Assembled Monolayers on Thermodynamics and Kinetics of Cytochrome *c* Electron-Transfer Reactions. *Coord. Chem. Rev.* **2000**, *209*, 263−331.

(2) Armstrong, F. A.; Wilson, G. S. Recent Development in Faradaic Bioelectrochemistry. *Electrochim. Acta* **2000**, *45*, 2623−2645.

(3) Jeuken, L. J. C. Conformational Reorganisation in Interfacial Protein Electron Transfer. *Biochim. Biophys. Acta* **2003**, *1604*, 67−76.

(4) Murgida, D. H.; Hildebrandt, P. Redox and Redox-Coupled Processes of Heme Proteins and Enzymes at Electrochemical Interfaces. *Phys. Chem. Chem. Phys.* **2005**, *7*, 3773−3784.

(5) Waldeck, D. H.; Khoshtariya, D. E. In *Modern Aspects of Electrochemistry. Applications of Electrochemistry and Nanotechnology in Biology and Medicine*; Elias, N., Ed.; Springer: New York, 2011; Vol. *52*, pp 105−238.

(6) Hopfield, J. J. Electron Transfer between Biological Molecules by Thermally Activated Tunneling. *Proc. Natl. Acad. Sci. U.S.A.* **1974**, *71*, 3640−3644.

(7) Marcus, R. A.; Sutin, A. N. Electron Transfer in Chemistry and Biology. *Biochim. Biophys. Acta* **1985**, *811*, 265−322.

(8) Chidsey, C. E. D. Free Energy and Temperature Dependence of Electron Transfer at the Metal−Electrolyte Interface. *Science* **1991**, *251*, 919−922.

(9) Weber, K.; Creager, S. E. Voltammetry of Redox-Active Groups Irreversibly Adsorbed onto Electrodes. Treatment Using Marcus Relation between Rate and Overpotential. *Anal. Chem.* **1994**, *66*, 3164−3172.

(10) Kuznetsov, A. M.; Ulstrup, J. *Electron Transfer in Chemistry and Biology*; Wiley: Chichester, U.K., 1999; pp 1−374.

(11) Smalley, J. F.; Feldberg, S. W.; Chidsey, C. E. D.; Lindford, M. R.; Newton, M. D.; Liu, Y. P. The Kinetics of Electron Transfer through Ferrocene-Terminated Alkanethiol Monolayers on Gold. *J. Phys. Chem.* **1995**, 13141−13149.

(12) Chi, Q.; Zhang, J.; Andersen, J. E. T.; Ulstrup, J. Ordered Assembly and Controlled Electron Transfer of the Blue Copper Protein Azurin at Gold (111) Single-Cristal Substrates. *J. Phys. Chem. B* **2001**, *105*, 4669−4679.

(13) Gray, H. B.; Winkler, J. R. Electron Tunneling through Proteins. *Q. Rev. Biophys.* **2003**, *36*, 341−372.

(14) Feldberg, S. W.; Sutin, N. Distance Dependence of Heterogeneous Electron Transfer through the Nonadiabatic and Adiabatic Regimes. *Chem. Phys.* **2006**, *324*, 216−225.

(15) Yokoyama, K.; Leigh, B. S.; Sheng, Y.; Niki, K.; Nakamura, N.; Ohno, H.; Winkler, J. R.; Gray, H. B.; Richards, J. H. Electron Tunneling through *Pseudonomas aureginosa* Azurins on SAM Gold Electrodes. *Inorg. Chim. Acta* **2008**, *361*, 1095−1099.

(16) Zusman, L. D. Outer-Sphere Electron Transfer in Polar Solvents. *Chem. Phys.* **1980**, *49*, 295−304.

(17) Zusman, L. D. The Theory of Transitions between Electronic States: Application to Radiatonless Transition in Polar Solvents. *Chem. Phys.* **1983**, *80*, 29−43.

(18) Rips, I.; Jortner, J. Dynamic Solvent Effects on Outersphere Electron Transfer. *J. Chem. Phys.* **1987**, *87*, 2090−2104.

(19) Beratan, D. N.; Onuchic, J. N. Adiabacity and Non-adiabacity in Bimolecular Outer-Sphere Charge Transfer Reaction. *J. Chem. Phys.* **1988**, *89*, 6195−6203.

(20) Weaver, M. J.; Mac-Manis, G. E. Dynamical Solvent Effects on Electron-Transfer Processes: Recent Progress and Perspectives. *Acc. Chem. Res.* **1990**, *23*, 294−300.

(21) Weaver, M. J. Dynamical Solvent Effects on Activated Electron-Transfer Reactions: Principles, Pitfalls and Progress. *Chem. Rev.* **1992**, *92*, 463−480.

(22) Zusman, L. D. Dynamical Solvent Effect in Electron Transfer Reaction. *Z. Phys.Chem.* **1994**, *186*, 1−29.

(23) Khoshtariya, D. E.; Dolidze, T. D.; Zusman, L. D.; Waldeck, D. H. Observation of the Turnover between the Solvent Friction (Overdamped) and Tunneling (Nonadiabatic) Charge-Transfer Mechanisms for a Au/Fe$(CN)_6^{3-/4-}$ Electrode Process and Evidence for a Freezing Out of the Marcus Barrier. *J. Phys. Chem. A* **2001**, *105*, 1818−1829.

(24) Wei, J.; Liu, H.; Khoshtariya, D. E.; Yamamoto, H.; Dick, A.; Waldeck, D. H. Electron-Transfer Dynamics of Cytocrome c: A Change in the Reaction Mechanism with Distance. *Angew. Chem., Int. Ed.* **2002**, *41*, 4700−4703.

(25) Schmickler, W.; Mohr, J. The Rate of Electrochemical Electron-Transfer Reactions. *J. Chem. Phys.* **2002**, *117*, 2867−2872.

(26) Khoshtariya, D. E.; Wei, J.; Liu, H.; Yue, H.; Waldeck, D. H. Charge-Transfer Mechanism for Cytocrome *c* Adsorbed in Nanometer Thick Films. Distinguishing Frictional Control from Conformational Gating. *J. Am. Chem. Soc.* **2003**, *125*, 7704−7714.

(27) Khoshtariya, D. E.; Dolidze, T. D.; Sarauli, D.; Van Eldik, R. High-Pressure Probing of a Changeover in the Charge-Transfer Mechanism for Intact Cytocrome *c* at Gold/Self-Assembled Monolayers Junctions. *Angew. Chem., Int. Ed.* **2006**, *45*, 277−281.

(28) Yue, H.; Khoshtariya, D. E.; Waldeck, D. H.; Grochol, J.; Hildebrandt, P.; Murgida, D. H. On the Electron Transfer Mechanism Between Cytocrome *c* and Metal Electrodes. Evidences for Dynamic Control at Short Distances. *J. Phys. Chem. B* **2006**, *110*, 19906−19913.

(29) Mishra, A. K.; Waldeck, D. H. A Unified Model for the Electrochemical Rate Constant that Incorporates Solvent Dynamics. *J. Phys. Chem. C* **2009**, *113*, 17904−17914.

(30) Khoshtariya, D. E.; Dolidze, T. D.; Van Eldik, R. Multiple Mechanisms for Electron Transfer at Metal/Self-Assembled Monolayer/Room-Temperature Ionic Liquid Junctions: Dynamical Arrest versus Frictional Control and Non-adiabaticity. *Chem.—Eur. J.* **2009**, *15*, 5254−5262.

(31) Khoshtariya, D. E.; Dolidze, T. D.; Shushanyan, M.; Davis, K. L.; Waldeck, D. H.; Van Eldik, R. Fundamental Signatures of Short- and Long-Rate Electron Transfer for the Blue Copper Protein Azurin at Au/SAM Junction. *Proc. Natl. Acad. Sci. U.S.A.* **2010**, *107*, 2757−2762.

(32) Sumi, H. Theory on Reaction Rates in Nonthermalized Steady States during Conformational Fluctuations in Viscous Solvents. *J. Phys. Chem.* **1991**, *95*, 3334−3350.

(33) Avila, A.; Gregory, B. W.; Niki, K.; Cotton, T. M. An Electrochemical Approach to Investigate Gated Electron Transfer Using a Physiological Model System: Cytochrome *c* Immobilized on Carboxylic Acid-Terminated Alkanethiol Self-Assembled Monolayers on Gold Electrodes. *J. Phys. Chem. B* **2000**, *104*, 2759−2766.

(34) Davidson, V. Protein Control of True, Gated and Coupled Electron Transfer Reactions. *Acc. Chem. Res.* **2008**, *41*, 730−738.

(35) Kranich, A.; Ly, H. K.; Hildebrandt, P.; Murgida, D. H. Direct Observation of the Gating Step in Protein Electron Transfer: Electric-Field-Controlled Protein Dynamics. *J. Am. Chem. Soc.* **2008**, *130*, 9844−9848.

(36) Kranich, A.; Naumann, H.; Molina-Heredia, F. P.; Moore, H. J.; Lee, T. R.; Lecomte, S.; De la Rosa, M. A.; Hildebrandt, P.; Murgida, D. H. Gated Electron Transfer of Cytochrome c_6 at Biomimetic Interfaces: A Time-Resolved SERR Study. *Phys. Chem. Chem. Phys.* **2009**, *11*, 7390−7397.
(37) Álvarez-Paggi, D.; Martin, D. F.; DeBiase, P. M.; Tenger, K.; Hildebrandt, P.; Martí, M. A.; Murgida, D. H. Molecular Basis of Coupled Protein and Electron Transfer Dynamics of Cytocrome *c* in Biomimetic Complexes. *J. Am. Chem. Soc.* **2010**, *132*, 5769−5778.
(38) Georg, S.; Kabuss, J.; Weidinger, I. M.; Murgida, D. H.; Hildebrandt, P.; Knorr, A.; Richter, M. Distance-Dependent Electron Transfer of Immobilized Redox Protein: A Statistical Physics Approach. *Phys. Rev. E* **2010**, *81*, 046101/1−046101/10.
(39) Álvarez-Paggi, D.; Meister, W.; Kuhlmann, U.; Weidinger, I.; Tenger, K.; Zimányi, L.; Rákhely, G.; Hildebrandt, P.; Murgida, D. H. Distetangling Electron Tunelling and Protein Dynamics of Cytocorme C through a Rationally Designed Surface Mutation. *J. Phys. Chem. B* **2013**, *117*, 6061−6068.
(40) Liu, H.; Yamamoto, H.; Wei, J.; Waldeck, D. H. Control of the Electron Transfer Rate between Cytochrome *c* and Gold Electrodes by the Manipulation of the Electrodés Hydrogen Bonding Character. *Langmuir* **2003**, 2378−2387.
(41) Davis, K. L.; Drews, B. J.; Yue, H.; Waldeck, D. H.; Knorr, K.; Clark, L. A. Electron Transfer Kinetics of Covalently Attached Cytochrome *c*/SAM/Au Electrode Assemblies. *J. Phys. Chem. C* **2008**, *7*, 3773−3784.
(42) Monari, S.; Battistuzzi, G.; Dennison, C.; Borsari, M.; Ranieri, A.; Siwek, J. M.; Sola, M. Factors Affecting the Electron Transfer Properties of Immobilized Cupredoxin. *J. Phys. Chem. C* **2010**, *114*, 22322−22329.
(43) Monari, S.; Battistuzzi, G.; Bortolotti, C. A.; Yanagisawa, S.; Sato, K.; Li, C.; Salard, I.; Kostrz, D.; Borsari, M.; Ranieri, A.; Dennison, C.; Sola, M. Understanding the Mechanism of Short-Range Electron Transfer Using an Immobilized Cupredoxin. *J. Am. Chem. Soc.* **2012**, *134*, 11848−11851.
(44) Harris, M. R.; Davis, D. J.; Durham, B.; Millet, F. Temperature and Viscosity Dependence of the Electron-Transfer Reaction between Plastocyanin and Cytochrome *c* Labeled with a Ruthenium (II) Bipyridine Complex. *Biochim. Biophys. Acta* **1997**, *1319*, 147−145.
(45) Khoshtariya, D. E.; Dolidze, T. D.; Seifert, S.; Sarauli, D.; Lee, G.; Van Eldik, R. Kinetic, Thermodynamic, and Mechanistic Patterns for Free (Unbound) Cytochrome *c* at Au/SAM Junctions: Impact of Electronic Coupling, Hydrostatic Pressure, and Stabilizing/Denaturing Additives. *Chem.—Eur. J.* **2006**, *12*, 7041−7056.
(46) Olloqui-Sariego, J. L.; Frutos-Beltrán, E.; Roldán, E.; De la Rosa, M. A.; Calvente, J. J.; Díaz-Quintana, A.; Andreu, R. Voltammetric Study of the Adsorbed Thermophilic Plastocyanin from *Phormidium laminosum* up to 90°C. *Electrochem. Commun.* **2012**, *19*, 105−107.
(47) Feio, M. J.; Navarro, J. A.; Teixeira, M. S.; Harrison, D.; Karlsson, B. G.; De la Rosa, M. A. A Thermal Unfolding Study of Plastocyanin from the Thermophilic Cyanobaterium *Phormidium laminosum*. *Biochemistry* **2004**, *43*, 14784−14791.
(48) Muñoz-López, F. J.; Frutos-Beltrán, E.; Díaz-Moreno, S.; Díaz-Moreno, I.; Subías, G.; De la Rosa, M. A.; Díaz-Quintana, A. Modulation of Copper Site Properties by Remote Residues Determines the Stability of Plastocyanins. *FEBS Lett.* **2010**, *584*, 2346−2350.
(49) Oevering, H.; Paddon-Row, M. N.; Heppener, M.; Oliver, A. M.; Cotsaris, E.; Verhoeven, J. W.; Hush, N. S. Long-Range Photoinduced Through-Bond Electron Transfer and Radiative Recombination via Rigid Nonconjugated Bridges: Distance and Solvent Dependence. *J. Am. Chem. Soc.* **1987**, *109*, 3258−3269.
(50) Smalley, J. F.; Frinklea, H. O.; Chidsey, C. E. D.; Linford, M. R.; Creager, S. E.; Ferraris, J. P.; Chalfant, K.; Zawodzinsk, T.; Feldberg, S. W.; Newton, M. D. Heterogeneous Electron Transfer Kinetics Ruthenium and Ferrocene Redox Moieties through Alkanethiol Monolayers on Gold. *J. Am. Chem. Soc.* **2003**, *125*, 2004−2013.
(51) Di Bilio, A. J.; Hill, M. G.; Bonander, N.; Karlsson, B. G.; Villahermosa, R. M.; Malmström, B. G.; Winkler, J. R.; Gray, H. B. Reorganization Energy of Blue Copper: Effects of Temperature and Driving Force on the Rates of Electron Transfer in Ruthenium-Osmium-Modified Azurins. *J. Am. Chem. Soc.* **1997**, *119*, 9921−9922.
(52) Solomon, E. I.; Szilagyi, R. K.; DeBeer-George, S.; Basumallick, L. Electronic Structures of Metal Sites in Protein and Models: Contributions to Function in Blue Copper Proteins. *Chem. Rev.* **2004**, *104*, 419−458.
(53) Cascella, M.; Magistrato, A.; Tavernelli, I.; Carloni, P.; Rothlisberger, U. Role of the Protein Frame and Solvent for the Redox Properties of Azurin from *Pseudonomas aureginosa*. *Proc. Natl. Acad. Sci. U.S.A.* **2006**, *103*, 19641−19646.
(54) LeBard, D. N.; Matyushov, D. V. Glassy Protein Dynamics and Gigantic Solvent Reorganization Energy of Plastocyanin. *J. Phys. Chem. B* **2008**, *112*, 5218−5227.
(55) Fawcet, W. R. *Liquids, Solutions and Interfaces*; Oxford University Press: New York, 2004.
(56) Ma, L.; Hass, M. A. S.; Vierick, N.; Kristenses, S. N.; Ulstrup, J.; Led, J. J. Backbones Dynamics of Reduced Plastocyanin from Cyanobacterium *Anabaena Variabilis*: Regions Involved in Electron Transfer Have Enhanced Mobility. *Biochemistry* **2003**, *42*, 320−330.
(57) Zhou, J. S.; Kostic, N. M. Gating of Photoinduced Electron Transfer from Zinc Cytochrome *c* and Tin Cytochrome *c* to Plastocyanin. Effects of Solution Viscosity on Rearrangement of the Metalloprotein Complex. *J. Am. Chem. Soc.* **1993**, *115*, 10796−10804.